Writing of internal gratings in optical glass with a femtosecond laser

Guanghua Cheng (程光华), Qing Liu (刘 青), Yishan Wang (王屹山), Lianjun Yu (于连军), Wei Zhao (赵 卫), and Guofu Chen (陈国夫)

State Key Laboratory of Transient Optics and Technology, Xi'an Institute of Optics and Precision Mechanics, Chinese Academy of Sciences, Xi'an 710068

Received October 9, 2003

The writing of an internal diffraction grating in optical glass plate is demonstrated using low-density plasma formation excited by a high-intensity femtosecond Ti:sapphire laser. The same diffraction efficiency at ± 1, ± 2, and 0 order is achieved by multiple layers writing. The dependences of diffractive efficiency on the irradiated energy, the speed of writing, the numerical aperture (NA) of the focusing objective, and materials are investigated in detail. The grating is birefringent. It is attributed to residual stress interaction between glass and femtosecond laser pulse.

OCIS codes: 050.1950, 140.3390, 320.7110, 220.4610.

Ultra-short laser pulse driven micro-explosions provide a unique method for creating micro-structures within high bandgap materials with minimal thermal damage. This ability to create three-dimensional (3D) objects with sub-micrometer precision may be useful for creating various types of periodic structures such as diffractive optical elements[1], photonic bandgap material[2], pattern gratings in fibers[3] and 3D data storage[4]. The technique is not limited to optically transparent materials, and can also be applied to semiconductors[5], ceramics[6] and biological tissues[7]. Recently, the fabrication of a diffraction grating with photo-induced refractive index modification in planar silica plate and optical sensitivity materials was demonstrated using holographic interference with a high-intensity femtosecond laser[8−10] and directly scanning a glass sample with focusing a relative low-intensity laser beam[11,12]. However, the holographic interference scheme requires high pulse energy (500 μJ, typical) as well as precision time delay due to a well-known fact that it is hard to make sure the interference of two laser beams in femtosecond time scale. Low stability and diffraction efficiency were Comparing with the first approach, the scanning scheme inquires relative low energy (500 nJ, typical) and simple experimental setup. But the recently reported refraction efficiency is very low due to high scattering in fused silica[13].

In this article, the writing of a high diffraction efficiency grating in planar fused silica, ZBaF15, K9, and ZK6 optical glass plates was demonstrated using low-density plasma formation excited by a high-intensity femtosecond Ti:sapphire laser. The gratings of uniform diffractive efficiency in ZBaF15, K9, and ZK6 optical glass plates have been achieved by multi-layer recording. We characterize the structural properties of these micrometer diameter refractive index changes in those optical glasses. Birefringence is attributed to residual stress interaction between glass and femtosecond laser pulse. A mechanism is proposed to explain the formation of different structures in the different materials.

The experimental setup, reported elsewhere[14,15], consists of four parts: femtosecond laser system at high pulse energy and low repetition rate, phase-contrast optical microscope for real-time monitor and imaging, and 3D scanner with nm order resolution. In detail, a home-built chirped pulse amplified Ti:sapphire laser pulse (up to 100 μJ in a 100 fs to 1 ps pulse, $1-5$ kHz repetition rate) is first passed through a spatial light filter (10-μm pinhole) in order to improve the laser beam quality and enlarge its diameter. A microscope objective (40× magnification, NA = 0.45 or 0.65) focuses the pulse into a sample. The glass plates are prepared in cubic shape with four optical surfaces to allow the laser-matter interaction zone to be observed from different orthogonal directions. A computer controlled three-axis translation stage (resolution of 100 nm at X and Y axis, 7 nm at Z axis) is used to move the sample between pulses.

For measuring the laser induced damage threshold, some optical glasses are used such as pure fused silica, borate crown, barium crown and lanthanum flint glasses, their trademarks in China are GJS1, K9, ZK6, LaF3 and ZF6, respectively. The laser beam was focused into the glass by an objective and the energy of the irradiated laser was adjusted through the attenuator. A digital (Nikon) camera, attached to a conventional phase-contrast optical microscope, was used to observe the grating after irradiation.

Figure 1 is a phase-contrast micrograph of a ZBaF15 optical glass grating making with a 3-μJ femtosecond laser with a NA = 0.45 objective. The lines are separated by 10 μm. The sample is moved with a speed of 500 μm/s. The periodic refractive index modulation of the grating is shown by integral of the refractive index of the grating. The diffraction efficiency of the grating was measured with He-Ne laser. Accordingly, the far-field diffraction pattern is given in the figure. The bottom graph gives the diffraction efficiency of the grating. The middle spot is order 0. The diffraction efficiency of the orders ± 1 is about 30% (normalized with respect to order 0).

Figure 2 shows a phase-contrast micrograph of a Zk6 optical glass grating encoding by the femtosecond laser with a NA = 0.65 objective. The distance between two lines is 2 μm. The sample is moved with a speed of 200 μm/s. From the far-field diffraction pattern of a

He-Neon laser beam and the diffraction efficiency of the grating, the intensity of the orders ± 1 is same as the order 0.

Figure 3 presents a far-field diffraction pattern of a 3-layer grating in K9 optical glass, encoding with a NA = 0.65 objective. The lines are separated by 2 μm, and the spacing between two adjacent layers is 50 μm.

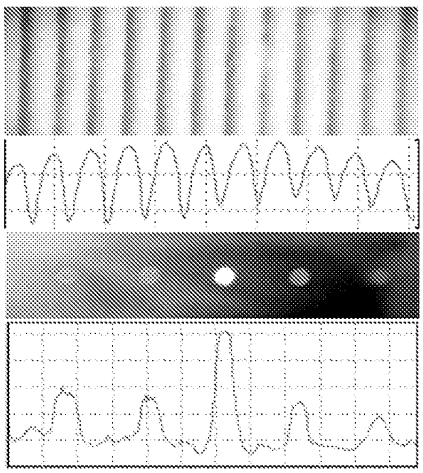

Fig. 1. Phase-contrast micrograph of a ZBaF15 glass grating encoding by a femtosecond laser (800 nm, 200 fs, 3 μJ, 1 kHz) with a NA = 0.45 objective (top). The lines are separated by 10 μm. The sample is moved with a speed of 500 μm/s. The periodic refractive index modulation of the grating (the second). Far-field diffraction pattern of a He-Ne laser beam (the third). Diffraction efficiency of the grating (bottom).

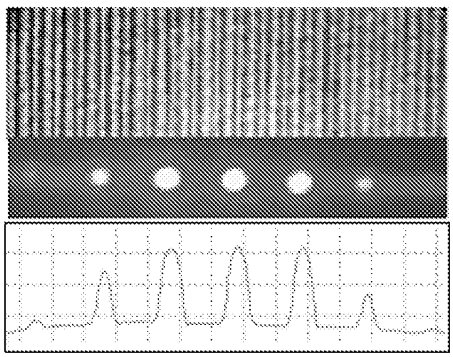

Fig. 2. Phase-contrast micrograph of a ZK6 optical glass grating encoding by the femtosecond laser with a NA = 0.65 objective (top). The lines are separated by 2 μm. The sample is moved with a speed of 200μm/s. Far-field diffraction pattern of a He-Ne laser beam (middle). Diffraction efficiency of the grating (bottom).

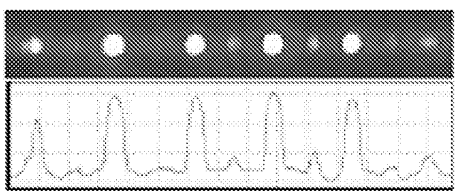

Fig. 3. Far-field diffraction pattern of a 3-layer grating in K9 optical glass, encoding with a NA = 0.65 objective (top). The lines are separated by 2 μm, and the spacing between two adjacent layers is 50 μm. Diffraction efficiency of the grating (bottom).

The sample is moved with a speed of 200 μm/s. The diffraction efficiencies of the orders ± 1, ± 2, and 0 are same.

Diffraction efficiency of a grating depends on the differences of refractive index and the depth of refractive index modulation. The writing parameters such as irradiated energy, the scanning speed, the recording material, and the recording layers are important for high diffraction efficiency. An excessive exposure (in our system, 1 μJ for fused silica, 0.5 μJ for other glass) leads to a scattering center along the written track, which leads to a decrease of the efficiency due to the result of physical damage. And there is a weak dependence of the diffraction efficiency on velocity when velocities are lower than 600 μm/s. The efficiency is saturated at the values of 200 μm/s, above the speeds of 600 μm/s it deceases sharply due to the fact that bits induced by laser pulse can not consist of line when the diameter of bit is about 600 nm, and the pulse repetition is 1 kHz (our writing conditions). At same exposure parameters, different materials obtain the different depth of refractive index modulation. So the efficiency is different. For example, 1-μJ energy with 0.65-NA focusing objective, the refractive-index modulation reaches to 40 μm for K9 optical glass, and 20 μm for fused silica.

Besides the selection of the materials, laser parameters such as beam quality and laser stability are also in consideration. In order to improve the laser beam, a two-step attenuation scheme was used to accurately control the pulse energy and remain circle laser beam inside sample. Instead of a neutral attenuator, a 10% beam splitter and a polarizer as analyzer were employed. It is well-known that a Gaussian laser beam becomes non-circular beam when it is through tunable neutral attenuator. And non-circular laser beam deteriorates seriously the quality for lithography.

We follow the result of L. Sudrie *et al.*[16] that a phase shift of each groove approximates to a supergaussian of order $\varphi(y) = \varphi_0 \exp(-y^2/r^2)^p p$, where φ_0 the maximum phase shift, r is the groove half-width. A best fit yields the values: $\varphi_0 = 1.946$, $r = 0.388$ μm, $p = 5$, accordingly $\Delta n = 4.38 \times 10^{-3}$ for the grating in K9 optical glass. Figure 4 presents the calculated grating diffraction patterns together with measured values obtained in K9 optical glass. By same way, $\varphi_0 = 0.892$, $r = 0.325$ μm, $p > 30$, $\Delta n = 4.1 \times 10^{-3}$ for the grating in Zk6 optical glass with the space of 2-μm periodicity.

In order to obtain the maximum diffraction efficiency at $+1$ or -1 order for super Gaussian phase-shift grating, the phase shift should be π. Due to $\varphi_0 = \Delta n \times d$, so there are two ways to increase the diffraction efficiency. One is to increase the modulation depth; another is to increase the refractive index changes. For simplicity, multi-layers recording is preferable. For energy of 1.5 μJ with 0.55-NA focusing objective (13-mm working distance), the modulation depth each layer is 50 μm in K9 optical glass. We recorded three layers with 50-μm spacing between two layers in K9 optical glass, shown in Fig. 3. In all, the modulation depth adds up to 150 μm. Accordingly, the diffraction efficiency increased apparently. The gratings of uniform diffractive efficiency in ZBaF15, K9, ZK6, and LaF3 optical glass plates have been achieved by multi-layer recording.

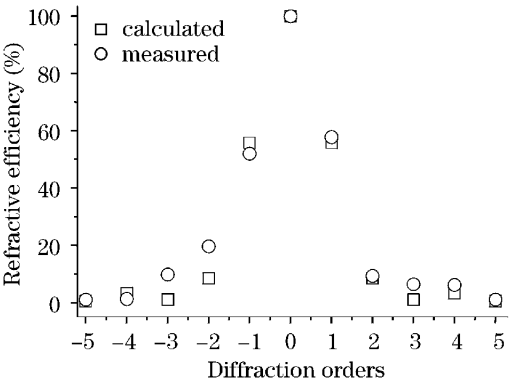

Fig. 4. Diffraction pattern inside a K9 glass (open circles) and the calculated diffraction patterns assuming super-Gaussian index profiles (open squares).

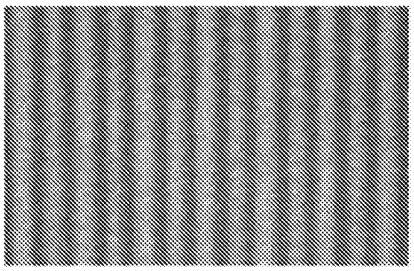

Fig. 5. The micro-photograph of grating observed by conventional phase-contrast microscopy with the birefringent scheme.

The grating in fused silica written by a 200-kHz femtosecond laser pulses is birefringent. J. Mills reported the anisotropic reflection of the grating in fused silica with 250-kHz repetition rate femtosecond laser[17]. To our knowledge, there is no report on birefringence and anisotropy in microstructure fabricated by low repetition rate femtosecond laser (for example, 1 kHz). We measured the birefringence of our grating with low repetition rate (1 kHz) femtosecond laser. The experimental setup is conventional phase-contrast microscopy with two cross polarizers.

Figure 5 is birefringent micro-photo of the grating of 10-μm-groove space in fused silica written by a 1-kHz femtosecond laser at 800 nm with a speed of 200 μm/s. A 0.45-NA objective and a 2-μJ pulse energy was used to write the grating. The micro-photograph observed by conventional phase-contrast microscopy is same as the Fig. 1 (top).

There are two factors that can lead to the birefringence. One is strain coming from the thermal effect interaction femtosecond laser pulse with glasses. Another is attributed to the crystalline, which has been verified by electron diffraction in silica fiber[18]. However, it is clearly shown that the width of each line in the grating is about 1 μm in phase-contrast microscopy, and is about $6 \sim 7$ μm in birefringence scheme. The diameter of optical spot is 2.4 μm for 0.45-NA objective; the line width is about 3 times as big as the optical spot. So it is impossible to induce crystallization at unexposed area.

On the other hand, heating is cumulated around focal volume in glass by multiphoton absorption of the femtosecond laser pulse. For example, a 1-μJ, 100-fs laser pulse leads to 3300 °C temperature increase in fused silica[19]. The local temperature change generates strain around the focal volume. Birefringence could be attributed to the strain tensor from the thermal effect. So the birefringence comes from thermal strain in unexposed area, and could come from crystallization and thermal strain in exposed area.

In conclusion, we demonstrate the writing of an internal diffraction grating in optical glass plates using low-density plasma formation excited by a high-intensity femtosecond Ti:sapphire laser. The dependences of diffractive efficiency on the irradiated energy, the speed of writing, the numerical aperture of the focusing objective, and materials are investigated in detail. The gratings of uniform diffractive efficiency in ZBaF15, K9, and ZK6 optical glass plates have been achieved by multilayer recording. And the grating is birefringent. We attribute the birefringence to stress interaction between glass and femtosecond laser pulse.

This work was supported by the National Natural Science Foundation of China under Grant No. 60078004 and the Director Foundation of State Key Laboratory of Transient Optics and Technology. G. Cheng's e-mail address is guanghuacheng@163.com.

References

1. E. N. Glezer and E. Mazur, Appl. Phys. Lett. **71,** 882 (1997).
2. J. J. Dubowski, Proc. SPIE **4088,** 55 (2000).
3. K. Itoh, T. Toma, and K. Yamada, Proc. SPIE **3801,** 158 (1999).
4. G. H. Cheng, Y. Wang, J. D. White, W. Zhao, and G. Chen, J. Appl. Phys. **84,** 2023 (2003).
5. T. V. Kononenko, S. V. Garnov, S. M. Pimenov, V. I. Konov, and F. Dausinger, Proc. SPIE **3343,** 458 (1998).
6. W. Chen, P. Xue, T. Yuan, and D. Y. Chen, Proc. SPIE **3934,** 87(2000).
7. T. Juhasz, G. Djotyan, F. H. Loesel, R. M. Kurtz, C. Horvath, J. F. Bille, and G. Mourou, Laser Physics **10,** 495 (2000).
8. Y. Li, K. Yamada, T. Ishizuka, W. Watanabe, K. Itoh, and Z. Zhou, Opt. Express **10,** 1173 (2002).
9. K. Kawamura, M. Hirano, T. Samiya, and H. Hosono, Appl. Phys. Lett. **81,** 1137 (2002).
10. K. Kawamura, N. Ito, N. Sarukura, M. Hirano, and H. Hosono, Rev. Sci. Instrum. **73,** 1711(2002).
11. S.-H. Cho, H. Kumagai, and K. Midorikawa, Nucl. Instr. Meth. Phys. Res. B **197,** 73 (2002).
12. L. Sudrie, M. Franco, B. Prade, and A. Mysyrowicz, Opt. Commun. **171,** 279 (1999).
13. J. Ihlemann, S. Muller, S. Puschman, D. Schafer, M. Wei, J. Li, and P. R. Herman, Appl. Phys. A **76,** 751 (2003).
14. G. Cheng, L. Yu, Y. Wang, Q. Liu, W. Zhao, and G. Chen, Chin. Opt. Lett. **1,** 225 (2003).
15. G. Cheng, J. D. White, Q. Liu, Y. Wang, W. Zhao, and G. Chen, Chin. Phys. Lett. **20,** 1283 (2003).
16. L. Sudrie, M. Franco, B. Prade, and A. Mysyrowicz, Opt. Commun. **191,** 333 (2001).
17. J. Mills, P. Kazansky, E. Bricchi, and J. Baumberg, Appl. Phys. Lett. **81,** 196 (2002).
18. I. W. Park, H. Ju, A. Avilov, S. H. Choh, E. K. Koh, S. H. Cho, H. Kumagai, and K. Midorikawa, Appl. Phys. Lett. **83,** 656 (2003).
19. A. M. Streltsov and N. F. Borrelli, J. Opt. Soc. Am. B **19,** 2496 (2002).